Nanoscale Advances

ROYAL SOCIETY OF CHEMISTRY

PAPER

View Article Online
View Journal | View Issue

Cite this: *Nanoscale Adv.*, 2022, **4**, 5109

Leaky membrane fusion: an ambivalent effect induced by antimicrobial polycations†

Shuai Shi,[a] Helen Fan[b] and Maria Hoernke *[a]

Both antimicrobial peptides and their synthetic mimics are potential alternatives to classical antibiotics. They can induce several membrane perturbations including permeabilization. Especially in model studies, aggregation of vesicles by such polycations is often reported. Here, we show that unintended vesicle aggregation or indeed fusion can cause apparent leakage in model studies that is not possible in most microbes, thus potentially leading to misinterpretations. The interactions of a highly charged and highly selective membrane-active polycation with negatively charged phosphatidylethanolamine/phosphatidylglycerol (PE/PG) vesicles are studied by a combination of biophysical methods. At low polycation concentrations, apparent vesicle aggregation was found to involve exchange of lipids. Upon neutralization of the negatively charged vesicles by the polycation, full fusion and leakage occurred and leaky fusion is suspected. To elucidate the interplay of leakage and fusion, we prevented membrane contacts by decorating the vesicles with PEG-chains. This inhibited fusion and also leakage activity. Leaky fusion is further corroborated by increased leakage with increasing likeliness of vesicle–vesicle contacts. Because of its similar appearance to other leakage mechanisms, leaky fusion is difficult to identify and might be overlooked and more common amongst polycationic membrane-active compounds. Regarding biological activity, leaky fusion needs to be carefully distinguished from other membrane permeabilization mechanisms, as it may be less relevant to bacteria, but potentially relevant for fungi. Furthermore, leaky fusion is an interesting effect that could help in endosomal escape for drug delivery. A comprehensive step-by-step protocol for membrane permeabilization/vesicle leakage using calcein fluorescence lifetime is provided in the ESI.

Received 18th July 2022
Accepted 24th October 2022

DOI: 10.1039/d2na00464j

rsc.li/nanoscale-advances

Introduction

Natural or biomimetic membrane-active polycations exert a wide range of functions in biology, as candidates for antimicrobial therapy, or in drug delivery technology. It is known that polycations can cause aggregation and fusion of membranes or lipid vesicles, especially if membranes are negatively charged[1,2] or their lipid composition supports fusion intermediates.[3–6] In studies that use membrane model vesicles, aggregation or fusion are often suspected or reported, mostly as unwanted side effects.[2,7,8] The associated problems for proper experiments and data analysis need to be prevented or corrected for (for example light scattering in spectroscopic methods). Additionally, a relation of leakage and fusion has been suspected[9–11] or proven[12,13] in several cases. Therefore, there is a risk for severe misinterpretation as we will illustrate in the current study.

Here, we show in the context of membrane permeabilization, *i.e.*, leakage that vesicle aggregation and fusion can be highly relevant for induced membrane perturbations. As representative polycation, the synthetic oligomer poly-NM designed for selective antifungal and antibacterial activity is used (Fig. 1, more details below). These kinds of biomimetic polymers and natural antimicrobial peptides are of practical importance as they might complement classical antibiotics and thus help combat resistant pathogens, hopefully in the near future. For developing and selecting these compounds, it is important to understand their activity, but also the mechanism behind their

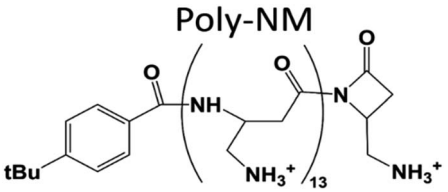

Fig. 1 Structure of poly-NM. Poly-NM is a homopolymer of β-"no methyl"-α-aminomethyl-β-lactam (NM) subunits.[29,30]

[a]*Chemistry and Pharmacy, Albert-Ludwigs-Universität, 79104 Freiburg i.Br., Germany. E-mail: Maria.Hoernke@bioss.uni-freiburg.de*

[b]*Leslie Dan Faculty of Pharmacy, University of Toronto, Toronto, Canada*

† Electronic supplementary information (ESI) available: Additional data and reference measurements (cryo-TEM, DLS, ITC, leakage, fusion assays). A comprehensive step-by-step protocol for membrane permeabilization/vesicle leakage using calcein fluorescence lifetime. See DOI: https://doi.org/10.1039/d2na00464j

selectivity. Membrane-active antimicrobials are believed to act by disturbing cell membrane integrity.

What combination of effects on membranes or other targets actually is required for antimicrobial killing needs elucidation. Apart from leakage, other effects such as changes in fusogenicity, changes in membrane properties that alter binding and potentially function of membrane proteins, or lateral electrostatic lipid clustering might also be relevant.[14–16] There are suggestions and evidence for many different leakage mechanisms[17] with more or less distinct characteristics. Hence oftentimes, vesicle leakage experiments are used to obtain systematic and mechanistic insight for antimicrobial activity, to assess drug delivery systems, endosomal escape, or the effect of membrane-active or pore-forming proteins, such as toxins. There are various options to characterize induced membrane permeabilization. Most commonly, a fluorescent dye or a dye–quencher pair is entrapped in large unilamellar vesicles (LUVs). If and how much of the vesicle content is released or retained is then assessed either by fluorescence intensity modulated by the extent of quenching[18] or *via* the fluorescence lifetime modulated by concentration-dependent self-quenching.[19]

For clarity in mechanistic studies, large unilamellar vesicles (LUVs) with defined binary lipid composition are preferred over natural lipid extracts or even natural membranes. Bacterial and fungal species differ in the composition of their membranes. Typically, microbial membranes and membrane models involve negatively charged lipids, often phosphatidylglycerol (PG) together with the zwitterionic lipid phosphatidylethanolamine (PE) amongst other lipids. Here, we use PE/PG in a 1 : 1 ratio. Usually, such negatively charged vesicles form stable colloids because the like-charged particles repel each other. The addition and binding of oppositely charged polyions can lead to vesicle aggregation by shielding of the vesicle charges or even direct cross-connection of vesicles. Vesicle aggregation itself should not induce leakage, but increased particle sizes cause turbidity and possibly sedimentation that can interfere with fluorescence experiments. Changes in light scattering/turbidity can also result from fusion which starts with aggregation. We will show that aggregation might involve exchange of membrane lipids and will thus use the term apparent aggregation. In full fusion, the membranes and content of the involved vesicles are combined to form a larger vesicle. (Unintentional) membrane fusion can be favoured in vesicles containing phosphatidylethanolamine lipids (PE) because the preference of PE with unsaturated chains (POPE) for negative spontaneous curvature facilitates rearrangements in the membrane leading to fusion intermediates. This is important because PE lipids are a prevalent component of microbial membranes and therefore a main constituent of microbial membrane models.

The details of the membrane fusion mechanism have been and are still under study. Briefly, the main energy barrier is thought to be the early step, namely vesicle aggregation and establishing close apposition with bilayer contact, more precisely, overcoming charge repulsion and removing hydration water.[20,21] Then, a tethered or docked state transfers into a more or less expanded hemifusion intermediate or fusion stalk. The opening of the fusion pore between the two fusing vesicles finally leads to full fusion. Importantly, fusion can be a tight or leaky process regarding entrapped cargo transferring to the outer medium through membrane defects. The characteristics of leaky fusion as leakage process, unfortunately, are thought to closely resemble other leakage mechanisms, namely asymmetric packing stress.[8,22] Asymmetric packing stress relies on a material imbalance in the outer and inner leaflet of a vesicle membrane.[23,24] Asymmetric packing stress seems relatively unselective comparing different lipid compositions and might, thus, be less or more desired for applications in antimicrobial therapy or drug delivery, for example. Therefore, confusing fusion with asymmetric packing stress can lead to misleading conclusions.

Both, in leakage or fusion, the activity of most membrane-active peptides or polymers relies on physical–chemical interactions driven by membrane properties, instead of specific binding sites. Therefore, the function of antimicrobial peptides can also be obtained with biomimetic polymers with positively charged and hydrophobic subunits.[25] Compared to natural peptides, the backbones of these short polymers can be more stable *in vivo* and thus would prolong circulation times that are otherwise compromised by proteolysis. In membrane-active polymers, there is a well-known spectrum between more hydrophobic, usually more active, but less selective polycations, and highly charged, less active but more selective polycations.[26] In a recent study, we examined a rather active/unselective antimicrobial polycation with significant hydrophobic surface.[22,27,28] This molecule is highly fusogenic but induces leakage by asymmetric packing stress in contrast to the present case.

Here, we investigate poly-NM, a candidate of the more selective, highly charged biomimetic polymers. Our model candidate poly-NM contains on average 13 subunits with a positively charged aminomethyl side chain (Fig. 1).[29] Poly-NM is selective for negatively charged over zwitterionic lipid compositions,[27,28] for bacterial species such as *B. subtilis* and *S. aureus*, and also for microbial fungi such as *C. albicans* and *C. neoformans*[29,30]. Poly-NM binds mainly by electrostatic interactions and induces membrane permeabilization above a threshold concentration as well as increased particle sizes indicating aggregation or fusion.[28]

For more details on the interplay of several effects involving membranes, we examined leakage and both vesicle aggregation and vesicle fusion. For this, a combination of biophysical methods is used: dynamic light scattering, cryo-transmission electron microscopy (cryo-TEM), isothermal titration calorimetry (ITC), two classical experiments to prove fusion in large unilamellar vesicles (LUVs), and leakage that is monitored thoroughly by fluorescence lifetime-based vesicle leakage experiments. We found a sequence of membrane effects depending on the poly-NM concentration. We took care to account for potential changes in light scattering as detailed in the methods section for each experiment.

We will present that apparent vesicle aggregation and vesicle fusion might not just be side effects, but can determine the outcome of vesicle leakage experiments and influence the

interpretation of leakage in view of antimicrobial activity or other therapeutic applications.

Experimental section

Materials

1-Palmitoyl-2-oleoyl-*sn*-glycero-3-phosphoethanolamine (POPE) and 1-palmitoyl-2-oleoyl-*sn*-glycero-3-phospho-(1′-*rac*-glycerol) (POPG, sodium salt) were purchased from Avanti Polar Lipids (Alabaster, AL, USA) as chloroform stock solutions. *N*-(Carbonyl-methoxypolyethylene glycol-2000)-1,2-distearoyl-*sn*-glycero-3-phosphoethanolamine (DSPE-PEG_{2000}, sodium salt) was kindly provided by Lipoid (Ludwigshafen, Germany) as powder. *N*-(7-Nitrobenz-2-oxa-1,3-diazol-4-yl)-1,2-dihexadecanoyl-*sn*-glycero-3-phosphoethanolamine (NBD-PE) and Lissamine™ rhodamine B 1,2-dihexadecanoyl-*sn*-glycero-3-phosphoethanolamine (Rho-DHPE) were both obtained as triethylammonium salt from Molecular Probes (Eugene, OR, USA). The fluorescence dyes calcein and 8-aminonaphthalene-1,3,6-trisulfonic acid (ANTS, disodium salt) as well as its quencher *p*-xylene-bis(*N*-pyridinium bromide) (DPX) were purchased from Sigma-Aldrich (St. Louis, MO, USA). All other chemicals and buffer substances were used of analytical grade as received from Carl Roth (Karlsruhe, Germany). Poly-NM was synthesized, purified, and quantified as previously described and a kind gift of the lab of Runhui Liu (East China University of Science and Technology, Shanghai, China).[29] Poly-NM was stored as lyophilized powder. For measurements, the concentration of stock solutions was 5 mg mL^{-1} (26 mM of poly-NM subunits). Ultrapure water produced by an Arium® Pro system (Sartorius AG, Goettingen, Germany) was used to prepare all the buffers and solutions. The standard MOPS buffer was composed of 25 mM MOPS (3-(*N*-morpholino)propane sulfonic acid) and 130 mM NaCl at pH 7.0. Moreover, 25 mM MOPS are used in all inside buffers with desired fluorescence dye and all buffers were adjusted with NaCl to 265 mOsmol kg^{-1} at pH 7.0.

Preparation and characterization of large unilamellar vesicles (LUVs)

Large unilamellar vesicles composed of POPE/POPG (1 : 1) and POPE/POPG/DSPE-PEG_{2000} (50 : 50 : 4 or 50 : 50 : 1) were prepared by thin-film hydration followed by 5 freeze–thaw cycles and 51 extrusions through an 80 nm polycarbonate membrane (Whatman International Ltd, Maidstone, UK). Lipid films of POPE/POPG (1 : 1) without or with DSPE-PEG_{2000} were prepared from the same stock chloroform solution of a POPE/POPG lipid mixture so that the POPE/POPG molar ratio is always identical.

Unless stated otherwise, especially for the fluorescence-based leakage or fusion assays, extruded LUVs (approximately 100 nm diameter) with the fluorescence labels mentioned were used at a total lipid concentration of 30 μM. For all vesicle preparations, the osmolality of the inside and outside buffers was adjusted with NaCl to 265 mOsmol kg^{-1}.

The lipid concentration of the LUV preparation was quantified by the Bartlett phosphate assay[31] and the *z*-average vesicle size (100–130 nm) and polydispersity index (PDI < 0.1) were determined using dynamic light scattering (DLS, Malvern Zetasizer Nano ZS, Worcestershire, UK).

For fluorescence leakage or fusion assays, the samples were incubated on a Thermoshaker (Hettich Benelux, Geldermalsen, Netherlands) in the dark at 400 U min^{-1} and 25 °C. The corresponding measurements were performed after various incubation times (10 min, 30 min, 1 h, 2 h, 5 h, 24 h) (see step-by-step protocol in the ESI†).

Cryo-TEM imaging

Cryo-TEM experiments were performed with the equipment (Leo 912 Ω-mega, Carl Zeiss, Oberkochen, Germany) and the experimental protocol as described.[22] 8–10 mM extruded LUVs composed of POPE/POPG (1 : 1) or POPE/POPG/DSPE-PEG_{2000} (50 : 50 : 4) were incubated for 1 day in standard MOPS buffer with and without the addition of poly-NM. Two different lipid/poly-NM subunits molar ratios (20 : 1 and 5 : 1) were examined.

Vesicle size (*z*-average diameter and intensity distribution) and polydispersity indices (PDI) were measured with dynamic light scattering (DLS) by 200-fold dilution of aliquots of the samples used for cryo-TEM with a Malvern Nano Zetasizer (Malvern, Worcestershire, UK).

The lipid concentration of LUVs required for the cryo-TEM experiments was 8–10 mM and the same samples were diluted 200 times (c_{lipid} = 40–50 μM) for the related DLS evaluation.

Isothermal titration calorimetry (ITC)

A MicroCal VP-ITC (Malvern Instruments, Malvern, UK) was used to characterize the binding of poly-NM to POPE/POPG LUVs with and without 4% PEG-lipids. The injection syringe was filled with 3 mM extruded LUVs composed of POPE/POPG (1 : 1) or POPE/POPG/DSPE-PEG_{2000} (50 : 50 : 4). 0.15 mM poly-NM solution was loaded in the sample cell. A repeating volume of 5 μL was injected with a stirring speed of 394 rpm and an equilibration time of 300 s at 25 °C. The reference power was 5 μcal s^{-1} and all samples were prepared in MOPS standard buffer.

The NITPIC software[32,33] was used for the analysis of raw data. A one set of sites binding model (MicroCal PEAQ-ITC Analysis Software, Malvern Instruments Ltd, Malvern, UK) was used to fit the integrated data describing the electrostatic interaction between positively charged poly-NM and negatively charged lipid vesicles.

Calcein fluorescence lifetime-based leakage assay

Dye leakage from vesicles was evaluated based on the determination of the fluorescence lifetime and related pre-exponential factors of the decay of calcein fluorescence using time-correlated single-photon counting (TCSPC) on a FluoTime 100 spectrometer (PicoQuant, Berlin, Germany)[19] and step-by-step protocol in the ESI.†

Briefly, 70 mM calcein (self-quenching at this concentration with a short fluorescence lifetime of ~0.4 ns (τ_E)) was loaded in LUVs composed of POPE/POPG (1 : 1) or POPE/POPG/DSPE-PEG_{2000} (50 : 50 : 1 or 50 : 50 : 4). 30 μM of calcein-

loaded LUVs were then added to poly-NM solutions or MOPS buffer (as negative control). Calcein that leaks and is diluted (down to ~5 μM) is no longer self-quenched and hence has a long lifetime of ~4 ns (τ_F). By a biexponential fit to calcein decay curves, the fluorescence lifetimes, the amount (corresponding pre-exponential factors B) of entrapped calcein (with subscripts E) and free calcein (with subscripts F) are obtained:

$$F(t) = B_F e^{-t/\tau_F} + B_E e^{-t/\tau_E}$$

Therefore, the total leakage efficiency (L_{total}) after the addition of poly-NM was derived as:

$$\text{Total calcein leakage efficiency } (L_{total}) = \frac{B_F - B_{F0}}{B_F - B_{F0} + Q_{stat} B_E}$$

where the subscript 0 corresponds to the negative control (in the absence of poly-NM) and Q_{stat} (=1.2) is static quenching factor for calcein.[19]

For addition experiments, 30 μM calcein-filled POPE/POPG vesicles are first preincubated with a range of poly-NM concentrations. After 30 min of preincubation, different types and also different amounts of LUVs are added to the sample: 30 μM calcein-filled LUVs, 30 μM buffer-filled LUVs (to a final c_{lipid} of 60 μM) or 300 μM buffer-filled LUVs (to a final c_{lipid} of 330 μM). The leakage experiment performed without any additional LUVs is used as a reference value. The total volume changes less than 1% in the case of 30 μM added vesicles or less than 5% if 300 μM vesicles are added. Therefore, we assume the polymer concentration to remain almost unchanged.

The excess leakage L_{excess} is defined with respect to the evolution of leakage without addition of LUVs.

For experiments with addition of buffer-filled LUVs, L_{excess} is:

$$L_{excess} \text{ (30 min after addition)} = L_{total} \text{ (30 min after addition)} - L_{total} \text{ (30 min sample without addition)}$$

with L_{total} (30 min after addition) being the measured value after adding of buffer-filled LUVs and L_{total} (30 min sample without addition) correcting for the expected continuing leakage of the pre-incubated vesicles.

For experiments with addition of calcein-filled LUVs, we need to correct for the newly added calcein, *i.e.* additional intact vesicles that also become leaky over time:

$$L_{excess} \text{ (30 min after addition)} = L_{total} \text{ (30 min after addition)} - \frac{1}{2} L_{total} \text{ (30 min sample without addition)} - \frac{1}{2} L_{total} \text{ (0 min just before addition)}$$

The last term quantifies the leakage expected for the newly added calcein-filled LUVs occurring over the first 30 minutes of their incubation with poly-NM (assumed identical to the leakage from −30 min to 0 min in the preincubation sample, depicted in black color in all panels of Fig. 6A–D). The factor $\frac{1}{2}$ in both terms results from doubling the calcein concentration alongside the lipid concentration.

Vesicle size (z-average diameter) and polydispersity indices (PDI) were measured with dynamic light scattering (DLS) on Malvern Nano Zetasizer (Worcestershire, UK) using aliquots after the leakage assay, *i.e.* after 24 h incubation of LUVs in the absence or presence of poly-NM.

NBD-rhodamine lipid mixing assay

The Förster resonance energy transfer (FRET) from NBD-labeled lipids to rhodamine-labeled lipids[34] was monitored on an LS 55 fluorescence spectrometer (PerkinElmer Inc., Norwalk, USA). The setting parameters and detailed protocol were as described.[22]

Briefly, LUVs are labeled with and without 0.5 mol% NBD-PE (donor) and 0.5 mol% Rho-DHPE (acceptor). For a typical lipid mixing assay, 30 μM extruded LUVs (corresponding to 6 μM labeled vesicles and 24 μM unlabelled vesicles, *i.e.* ratio of labeled/unlabeled vesicles is 1 : 4) were added to poly-NM solutions or MOPS buffer (as negative control).

Lipid mixing efficiency in the presence of poly-NM was derived as:

$$\text{Lipid mixing efficiency} = \frac{R - R_0}{R_\infty - R_0}$$

$$R = \frac{I_{520}}{I_{580}}$$

R is the ratio of the maximum fluorescence intensities of NBD (I_{520}) and rhodamine (I_{580}) in the presence of poly-NM. The subscripts 0 and ∞ correspond to the negative control (in the absence of poly-NM) and positive control (in the presence of 1 v/v% TX100), respectively. Because the simple NBD intensity could be critically influenced by changes in light scattering due to increased particle sizes, the ratio of FRET-pair intensity (R) is analyzed, assuming no or only a minor wavelength-dependence of scattering issues. Note that we use two types of reference values: direct addition of TX100 to solubilize FRET-lipid labeled LUVs into micelles (a common reference for entirely suppressed FRET, data are shown in Fig. 6) and LUVs prepared separately containing only 1/5 of FRET labels (each 0.1% of NBD and Rho, Fig. S5†) for an estimated value reflecting extensive lipid mixing.

Moreover, since the FRET partners are located in the same LUV, simple aggregation of vesicles should not influence FRET results.[35]

ANTS/DPX content mixing assay

Based on the concentration-dependent collisional quenching of ANTS by DPX, the mixing of internal content upon vesicle fusion[36] was determined with an LS 55 fluorescence spectrometer (PerkinElmer Inc., Norwalk, USA).

Briefly, LUVs were filled with either 25 mM ANTS (dye) or 90 mM DPX (quencher), respectively. For the content mixing assay, a mixture of ANTS-filled and DPX-filled vesicles (30 μM

total lipid concentration with a mixing ratio of 1 : 1) was injected into poly-NM solutions or MOPS buffer (as negative control, *i.e.* 0% content mixing). Content mixing efficiency in the presence of poly-NM was calculated as:

$$\text{Content mixing efficiency} = \frac{I_0 - I}{I_0 - I_{100}}$$

where I is the corrected fluorescence intensity of ANTS at 525 nm in the presence of poly-NM. The subscript 0 corresponds to the negative control (in the absence of poly-NM). As positive control (subscript 100, *i.e.* 100% content mixing), LUVs were prepared with a co-encapsulated mixture of 12.5 mM ANTS and 45 mM DPX.

To correct for light scattering, changes in fluorescence intensity of ANTS-filled vesicles incubated with poly-NM and buffer-filled LUVs were recorded under identical incubation conditions,[37] so that, I was then corrected as:

$$I = I_{(\text{ANTS LUVs and DPX LUVs with poly-NM})} \frac{I_{(\text{ANTS LUVs and buffer LUVs})}}{I_{(\text{ANTS LUVs and buffer LUVs with poly-NM})}}$$

Results and discussion

The apparent vesicle aggregation and fusion induced by poly-NM are inhibited by PEG-lipids

Like many other antimicrobial compounds, the polycation poly-NM was examined for its activity inducing membrane permeabilization.[27,28] However, poly-NM not only induces leakage, but also increased particle sizes and broader distributions of particle sizes were found.[28] Usually, such behavior is ascribed to vesicle aggregation or/and vesicle fusion and reported as side effects. It likely results from colloidal instability upon neutralization of negatively charged vesicles by the positively charged polycations. In order to elucidate the changes in the sample, we recorded cryo-TEM images and performed dynamic light scattering (DLS).

The original LUVs composed of POPE/POPG (1 : 1) with a *z*-average size of 109 nm and PDI of 0.08 are well dispersed as uniform spheres throughout the buffer solution in the absence of poly-NM (Fig. 2A and B black data, additional cryo-TEM images in Fig. S1†). Some angular LUVs are also observed (Fig. 2A), probably because of lipid shape-associated packing defects in the binary mixture of POPE and POPG.

With the addition of poly-NM to POPE/POPG LUVs, significant apparent aggregation of vesicles was observed together with large, apparently fused vesicles (Fig. 2A). Moreover, DLS measurements confirmed large particles of several hundred nanometres in diameter and a significant increase in PDI (Fig. 2B). The two different lipid/poly-NM molar ratios result in slightly different effects: at the lower poly-NM concentration (lipid/poly-NM subunits ratio = 20 : 1, charge ratio $R_c = 10$), only apparently aggregated vesicles with a slight increase of *z*-average size were observed (Fig. 2). Large fused particles in TEM images and increased particles sizes of approximately 1000 nm in DLS data appeared only at high poly-NM concentration (lipid/poly-NM subunits ratio = 5 : 1, charge ratio $R_c = 2.5$) (Fig. 2). Thus, poly-NM seems to induce aggregation of vesicles and fusion in a concentration-dependent manner. Poly-NM also induced vesicle aggregation of giant unilamellar vesicles (GUVs).[28]

For more details on the aggregation or fusion behavior of PE/PG with the polycations, we intended to prevent these effects. Lipids with poly(ethylene glycol) (PEG) anchored to their head groups can form a steric barrier at the surface of liposomes that prevents vesicle aggregation[38] and vesicle fusion.[39] As proposed by Kenworthy *et al.*,[40] we added 4 mol% DSPE-PEG_{2000} during the preparation of POPE/POPG LUVs. At this concentration of PEG-lipids, the PEG-chains are supposed to adopt a 'mushroom' conformation covering the liposome surface.[40–42] Otherwise, small antimicrobial peptides or polymers should still be able to approach the lipid bilayer so that the binding should not be much affected.

Like the PEG-free vesicles, the well-dispersed POPE/POPG/DSPE-PEG_{2000} LUVs are mostly spherical with a low PDI (0.06) and a comparable size (*z*-average: 99 nm). In cryo-TEM images, there is no significant difference between PEG-ylated vesicles in the absence or presence of poly-NM. In particular, no fused vesicles or aggregation of vesicles are observed (Fig. 2 and S1†) even at the higher poly-NM concentration (lipid/poly-NM ratio of 5 : 1) (*z*-average: 117 nm and PDI: 0.1). This indicates an efficient inhibition of vesicle aggregation and vesicle fusion by PEG-lipids.

After having established, both, apparent vesicle aggregation and vesicle fusion, we need to understand how these processes affect vesicle leakage. For this, we compare binding, vesicle leakage, and vesicle aggregation or fusion in PEG-free and PEGylated vesicles. Finally, the impact of increasing the likeliness of vesicle aggregation and fusion on leakage activity will be examined at higher lipid concentration.

The presence of PEG-lipids in vesicles changes polymer-vesicle binding only slightly

The most trivial possibility to explain the suppressed apparent aggregation and fusion might be that binding of poly-NM to the lipid layer is disturbed by the PEG-chains. Therefore, we explored binding using isothermal titration calorimetry in the absence[28] and presence of PEG-lipids in the vesicles.

Heats of titration of 3 mM POPE/POPG LUVs to 0.15 mM poly-NM are depicted in Fig. 3. The binding parameters were obtained using a binding model with one set of sites accounting for the electrostatic interactions between positively charged poly-NM subunits and negatively charged PG lipid head groups.

Both, binding of poly-NM to LUVs without[28] or with 4 mol% DSPE-PEG_{2000} results in identical exothermic heats ($\Delta H_B = -1.4 \pm 0.2$ kJ mol^{-1}), indicating that the mode of binding is relatively unaffected. The stoichiometry of poly-NM subunits per charged lipid, b decreases from 1.2 ± 0.1 in PEG-free vesicles to 0.7 ± 0.1 in PEG-ylated vesicles. This decrease can be explained by the different leakage activity discussed below. Without PEG-lipids, the polycations probably also bind to the inner lipid leaflet of the vesicles, but in the presence of PEG-lipids, the inner leaflet may not participate in binding.

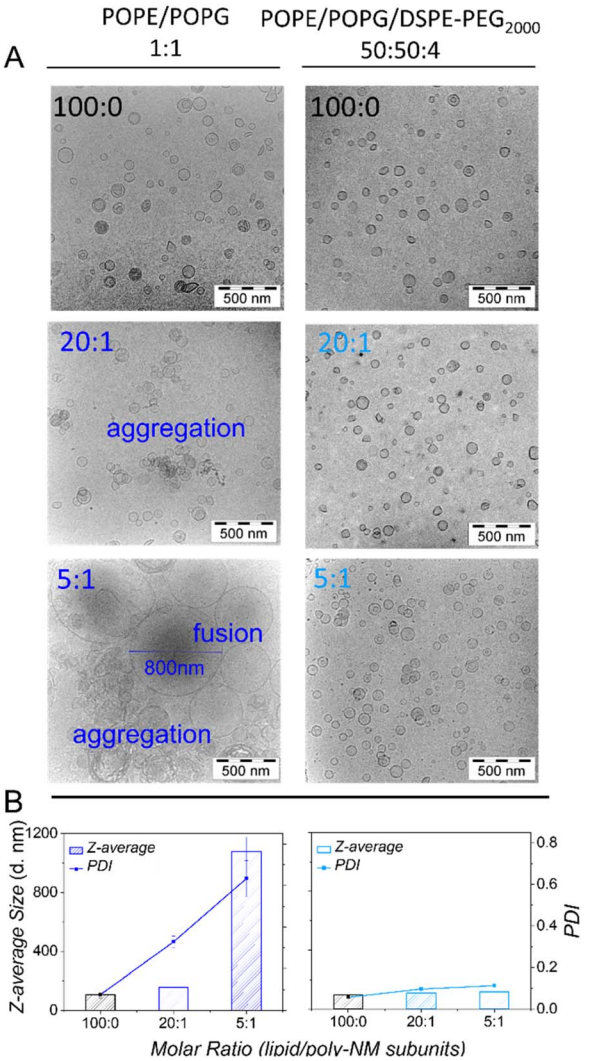

Fig. 2 Cryo-TEM images (A) and DLS results (B) of samples initially containing extruded LUVs composed of POPE/POPG (1 : 1) (left panel) or POPE/POPG/DSPE-PEG_{2000} (50 : 50 : 4) (right panel) in the absence (black) and presence (dark blue or light blue) of poly-NM. The lipid/poly-NM subunits molar ratio is indicated. For additional cryo-TEM images see Fig. S1.† 8–10 mM extruded LUVs were incubated with or without poly-NM for 1 day for cryo-TEM and diluted 200-fold for DLS. (25 mM MOPS; 130 mM NaCl; pH 7.0).

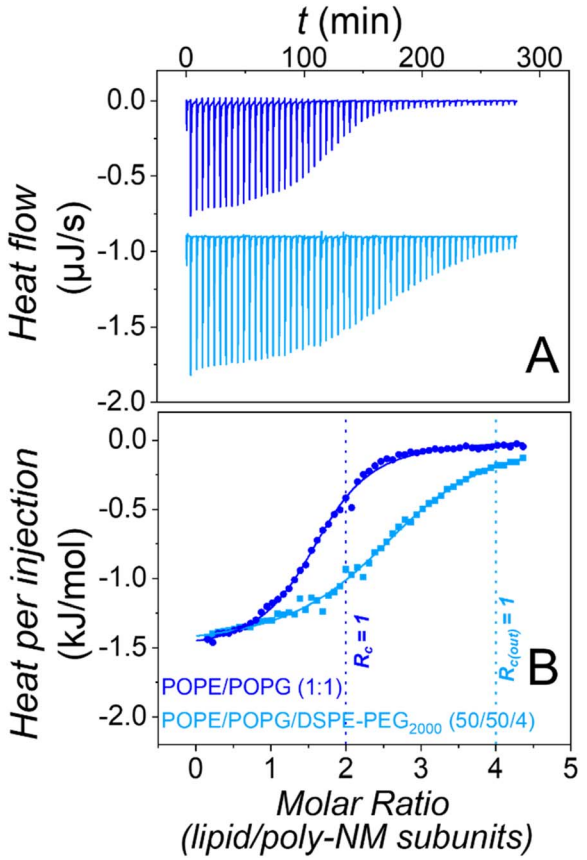

Fig. 3 ITC of poly-NM interacting with extruded LUVs composed of POPE/POPG (1 : 1) (dark blue) and POPE/POPG/DSPE-PEG_{2000} (50 : 50 : 4) (light blue). 3 mM liposomes were repeatedly injected into 0.15 mM poly-NM with an injection volume of 5 μL. Heat flows (A) and the corresponding integrated heats per injection (B) are shown. Solid lines in (B) show a fit using a binding model with one set of sites. The vertical dotted line represents the theoretical charge saturation ratio ($R_c = 1$) of POPE/POPG LUVs and poly-NM charges. The data of POPE/POPG (1 : 1) (dark blue) is reproduced from ref. Shi *et al.* 2021 with permission from the PCCP Owner Societies. (25 mM MOPS; 130 mM NaCl; pH 7.0; 25 °C).

Moreover, the apparent binding constant (K_B) decreases from 120 ± 10 mM^{-1} without PEG-lipids to 85 ± 10 mM^{-1} with PEG-lipids. This might indicate effects that are missing when vesicle aggregation or vesicle fusion are prevented in the presence of PEG-lipids.

In summary, the presence of DSPE-PEG_{2000} in POPE/POPG vesicles alters the presumably mainly electrostatic binding of poly-NM to PE/PG vesicles only marginally, showing that the interfacial PEG_{2000} does not disturb the approach and binding of poly-NM to the membrane. Direct binding of poly-NM to the PEG-chains is not expected and significant direct binding of poly-NM to soluble PEG_{2000} was excluded (Fig. S2†). Similarly, the presence of PEG-lipids in vesicles has almost no influence on melittin binding to membranes.[43]

Decreased bilayer–bilayer contacts: leakage induced by poly-NM is completely prevented in the presence of PEG-lipids

Vesicle aggregation and vesicle fusion can cause turbidity that may interfere with the determination of leakage.

We use a leakage assay based on the fluorescence lifetime of self-quenching calcein entrapped in vesicles.[19] A step-by-step protocol for this method is provided in the ESI.† These fluorescence-lifetime-resolved measurements are more independent of absolute fluorescence intensities, and thus turbidity, compared to the more common steady-state measurements. We confirmed that both calcein and ANTS/DPX leakage assays yield leakage in very good agreement (Fig. S3†). Furthermore, vesicle aggregation or fusion may also lead to types of leakage that are regarded as artefacts in the context of antimicrobial activity. Therefore, we carefully re-evaluated leakage behavior in the absence and presence of PEG-lipids.

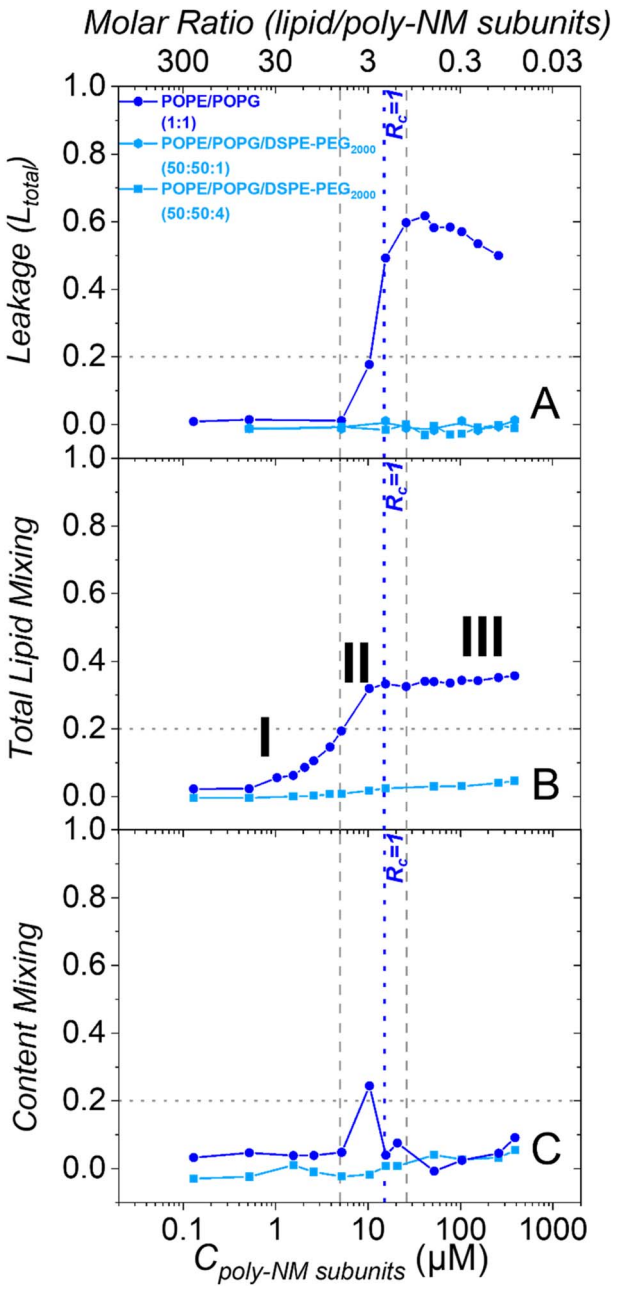

Fig. 4 Leakage, lipid mixing, and content mixing of extruded LUVs composed of POPE/POPG (1 : 1) (dark blue) or POPE/POPG/DSPE-PEG_{2000} (50 : 50 : 1 or 50 : 50 : 4) (light blue) in the presence of poly-NM. (A) Leakage based on calcein fluorescence lifetime. (B) Total lipid mixing based on FRET of NBD-PE to Rho-DHPE. (C) Content mixing assay based on quenching of ANTS fluorescence by DPX. Poly-NM subunits concentrations and lipid/poly-NM subunits molar ratio are indicated in the bottom and top axis, respectively. Lines are guides to the eye and used for the comparison of different assays. The vertical dotted line represents the theoretical charge saturation ratio ($R_c = 1$). 30 μM liposomes (initially 100–130 nm) are incubated with poly-NM for 1 h in MOPS buffer (25 mM MOPS; 130 mM NaCl; pH 7.0; 25 °C). Leakage data of POPE/POPG (1 : 1) vesicles in (A) is taken from ref. Shi *et al.* 2021 with permission from the PCCP Owner Societies.

As reported before, in the absence of PEG-lipids, poly-NM induces leakage of calcein from POPE/POPG LUVs starting above 5 μM (Fig. 4A).[28] Leakage reaches a constant leakage value above a threshold polymer concentration close to charge neutrality ($R_c = 1.0$ at 15 μM), *i.e.,* poly-NM does not induce more leakage at further increased concentrations (16–260 μM).[28] However, this plateau of leakage rises over time (Fig. S4A†).[28] Moreover, the comparison of theoretical to experimental data suggests that for the shorter incubation times up to approximately one hour, the leakage events are characterized as all-or-none (Fig. S4B†). For some of the vesicles, all entrapped calcein equilibrates at once, while other vesicles are not affected at all. At longer incubation times, leakage seems to occur more gradually, *i.e.,* the entrapped dye seems only partially diluted (Fig. S4B†).[28]

The leakage behavior induced by poly-NM changes dramatically when the vesicles contain additional PEG-lipids. Poly-NM does not induce any leakage up to at least 500 μM in POPE/POPG/DSPE-PEG_{2000} vesicles (PE/PG 1 : 1 plus 1% or 4% PEG-lipid) until 5 h (Fig. 4A and S4C, D†). Even with only 1% PEG-lipid, there is no significant leakage. There is no effect of an equivalent amount of soluble $mPEG_{2000}$ on the leakage behavior (Fig. S4E and F†).

Poly-NM induces apparent aggregation involving lipid mixing/fusion intermediates that is prevented by PEG-lipids

Cryo-TEM images indicate vesicle fusion (Fig. 2), but require much higher lipid concentrations (8–10 mM) than leakage experiments (30 μM). For direct comparison of leakage to potential fusion and for a better distinction of vesicle aggregation and vesicle fusion, two fluorescence-based fusion assays examining lipid mixing and content mixing were performed at an identical concentration of PEG-free and PEGylated LUVs.

First, we used Förster resonance energy transfer (FRET) to distinguish vesicle aggregation (contact of separate bilayers) from full membrane fusion or fusion intermediates (*i.e.* stalks or hemi-fusion) or apparent aggregation involving lipid exchange or mixing.

For quantifying lipid mixing, an excess of LUVs without fluorescence labels is mixed with LUVs containing a FRET-pair of head-group-labeled lipids (0.5% NBD-PE as FRET-donor and 0.5% Rho-DHPE as FRET-acceptor) (unlabeled : labeled = 4 : 1).[34] Upon full membrane fusion or formation of continuous fusion intermediates, the FRET pair is diluted with the additional unlabeled membrane lipids. Thus, the distance between donor and acceptor increases, resulting in a decrease in FRET efficiency.[35] Because absolute fluorescence intensity could be critically influenced by changes in light scattering, the ratio of FRET-pair intensity (R) is analyzed, assuming no or only a minor wavelength-dependence of scattering issues. Upon vesicle aggregation with only peripheral contact of separate membrane bilayers, no change in lipid mixing efficiency is expected.[35] Moreover, two references for quantifying lipid mixing are used (see details in methods and Fig. S5†).

In POPE/POPG LUVs without PEG-lipids, poly-NM induces lipid mixing at lower concentrations (0.5–16 μM) compared to

leakage (5–25 μM) (Fig. 4B). At poly-NM concentrations above $R_c = 1$, there is a plateau value of lipid mixing which slightly rises over time (Fig. S6A†). At the plateau, the lipid mixing efficiency remains approximately 0.4 with respect to the reference (micellization with Triton X). 0.4 is also the theoretical maximum value expected for vesicle fusion (also confirmed by Ca^{2+}-induced fusion, Fig. S6C†). This means that instead of causing vesicle aggregation with peripheral membrane contacts only, poly-NM induces fusion or fusion intermediates involving mixing of lipids or otherwise facilitates lipid exchange.

As described above, the presence of 4 mol% DSPE-PEG_{2000} in POPE/POPG vesicles impeded vesicle fusion completely at conditions used for cryo-TEM. Also at polymer concentrations up to 390 μM, poly-NM induced no perceivable lipid mixing (<5%) in POPE/POPG/DSPE-PEG_{2000} (50 : 50 : 4) LUVs up to 24 h (Fig. 4B and S6B†). Therefore, 4 mol% PEG-lipid is probably sufficient to completely prevent bilayer–bilayer contacts, *i.e.*, both vesicle aggregation and vesicle fusion are inhibited in the presence of poly-NM.

Full vesicle fusion and leakage upon charge neutralization are prevented by PEG-lipids

Strictly, for lipid mixing, already increased lipid exchange, fusion intermediates or hemifusion suffice. Hence, lipid mixing alone is no proof of full fusion. Another common fusion assay determines if also the internal aqueous contents mix between fusing vesicles, proving full fusion. For that, we performed a widely used fluorescence assay based on quenching of the soluble dye ANTS by DPX.[36] Briefly, ANTS and DPX are loaded in distinct LUVs at suitably high concentrations and these two types of LUVs are mixed (1 : 1) and incubated with the suspected fusion-active polycation.

There are several possible results: if LUVs do only aggregate or experience only hemifusion, there are no changes in ANTS intensity. If two or more LUVs are fully fused and the vesicle limiting membrane is tight during this process, highly concentrated DPX mixes with ANTS and quenches its fluorescence inside the combined vesicle lumen. In case leakage occurs, however, ANTS cannot be quenched, because DPX is too diluted. In leaky vesicles, the results of the content mixing assay are then the sum of fusion and leakage, and content mixing cannot always be quantified. Furthermore, it has to be noted that the efficiency of content mixing is determined using absolute fluorescence intensity and therefore can be affected by changes in light scattering. We corrected the data as detailed in the methods section[37] (Fig. S8†).

The content mixing observed after the addition of poly-NM to POPE/POPG LUVs without PEG-lipids progresses in an interesting way over the concentration range (Fig. 4C). At low poly-NM concentrations up to 5 μM, there is no content mixing even though lipid mixing, but no leakage is observed. At approximately 10 μM, there is a maximum content mixing efficiency. At higher concentrations, content mixing is reduced to a constant plateau value independent of poly-NM concentration, probably caused by leakage of DPX and/or ANTS. These findings agree with full vesicle fusion at polymer concentrations close to $R_c = 1$ that is accompanied by leakage.

Using PEG-ylated vesicles, there is no significant content mixing induced by poly-NM (<5%, Fig. 4C) and also until 24 h (Fig. S9†). This is as expected, since the incorporation of 4% PEG-lipids into POPE/POPG vesicles already prevented lipid mixing completely.

Dynamic light scattering confirms an increase in particle sizes and the polydispersity of 30 μM POPG/POPE vesicles depending on the concentration of poly-NM (Fig. 5). Like lipid mixing, the process starts at 1 μM poly-NM subunits. Particle sizes become huge and variable at charge neutralization ($R_c = 1$, Fig. 5). If PEG-lipids are incorporated into the vesicles, particle sizes remain in the same range as directly after preparation. This is consistent with cryo-TEM, lipid mixing, and content mixing results.

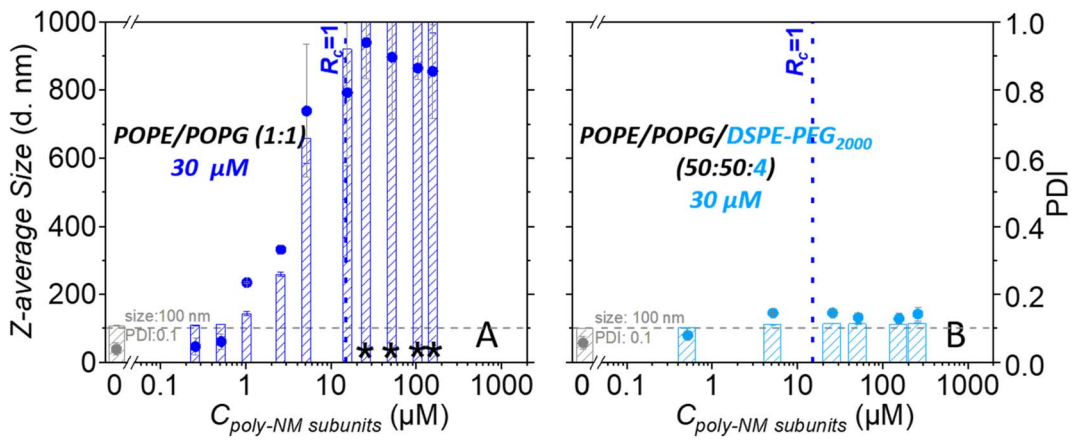

Fig. 5 Dynamic light scattering: particle size (*z*-average diameter, bar graph) and polydispersity indices (PDI, dot diagram) of 30 μM extruded LUVs composed of POPE/POPG (1 : 1) (dark blue) and POPE/POPG/DSPE-PEG_{2000} (50 : 50 : 4) (light blue) upon addition of poly-NM. Data in gray represent LUVs in the absence of poly-NM. Particle sizes larger than 1000 nm are marked by an asterisk. All data were recorded using aliquots after the calcein leakage assay reported below, *i.e.* after 24 h incubation of LUVs in the absence or presence of poly-NM. Some data in panel A are taken from Shi *et al.* 2021 with permission from the PCCP Owner Societies. (30 μM lipids; 25 mM MOPS; 130 mM NaCl; pH 7.0; 25 °C).

Increased bilayer–bilayer contacts increase leakage and indicate leaky fusion as leakage mechanism

Next, we increased the likeliness of bilayer–bilayer contacts by adding vesicles to a sample of vesicles preincubated with poly-NM and already some leakage.

For this, additional buffer-filled or calcein-filled vesicles were added to the initial 30 μM calcein-filled vesicles after 30 min preincubation with a range of poly-NM concentrations (Fig. 6). All vesicles are POPE/POPG (1 : 1). In the first two experiments, calcein-filled or buffer-filled LUVs were added doubling the lipid concentration to a final c_{lipid} of 60 μM (Fig. 6B and C). Third, 10 times the original amount of buffer-filled LUVs was added yielding a final c_{lipid} of 330 μM (Fig. 6D). Leakage is examined before (*i.e.* after 30 min of preincubation) and after the addition of LUVs.

At the time of vesicle addition, the preincubated samples exhibited approximately 50% total leakage starting at a threshold concentration close to $R_{c,30\ \mu M} = 1$ (15 μM poly-NM subunits) (Fig. 4A and 6). The leakage curves then exhibit the typical plateau or a slight apparent decrease of leakage with increasing poly-NM concentrations. In order to ensure meaningful comparison, for each addition experiment, the leakage of the exact same preincubated vesicle sample is depicted as black reference data and used for analysis. In the following paragraph and figures, the time point of adding LUVs is defined as t = 0 min for the total sample. The preincubation of the initial vesicles (30 μM) thus started at −30 minutes.

Upon addition of 30 μM LUVs, the general shape of the leakage curve remains qualitatively the same with a threshold and plateau (Fig. 6B and C). Upon addition of a tenfold excess of vesicles (300 μM), leakage stops which results in a constant plateau value. Only at high poly-NM concentrations, additional leakage occurs (Fig. 6D).

To evaluate whether leakage activity changes with the number of vesicles in the sample volume, we consider L_{excess}, the excess leakage (Fig. 6E, see methods for details). Briefly, if leakage activity continues independently of the vesicle number, $L_{excess} = 0$. Positive L_{excess} indicates increased leakage, *i.e.*, a dependence on the vesicle number. Negative L_{excess} would indicate a decrease in leakage activity of poly-NM after the addition of vesicles.

In all three addition experiments, L_{excess} becomes negative at $R_{c,30\ \mu M} = 1$ of the original sample and up to the new $R_c = 1$ (Fig. 6E). At poly-NM concentrations at the respective new $R_c = 1$ after the addition, an increase in leakage, *i.e.* a positive L_{excess} is observed in all experiments (Fig. 6E). The effect is most easily observed when a ten-fold excess of vesicles is added (300 μM), resulting in a constant leakage value (L_{total}) (Fig. 6D) and a negative L_{excess} between $R_{c,30\ \mu M} = 1$ and $R_{c,330\ \mu M} = 1$ (Fig. 6E).

Note that both, L_{total} in the original experiment and L_{excess} display leakage within 30 minutes of incubation/after addition.

Leaky membrane fusion: an ambivalent leakage mechanism

We think that leaky fusion is the mechanism by which poly-NM induces leakage in PE/PG vesicles. This conclusion is not straightforward. Here, we will discuss the three indications we collected: first, the sequence of effects that was established comparing leakage and fusion assays. Second, the response of these effects to a decrease in bilayer–bilayer contacts by decorating the vesicles with PEG-lipids. Third, the changes in leakage behavior upon the increase of potential bilayer–bilayer contacts by addition of further vesicles after preincubation.

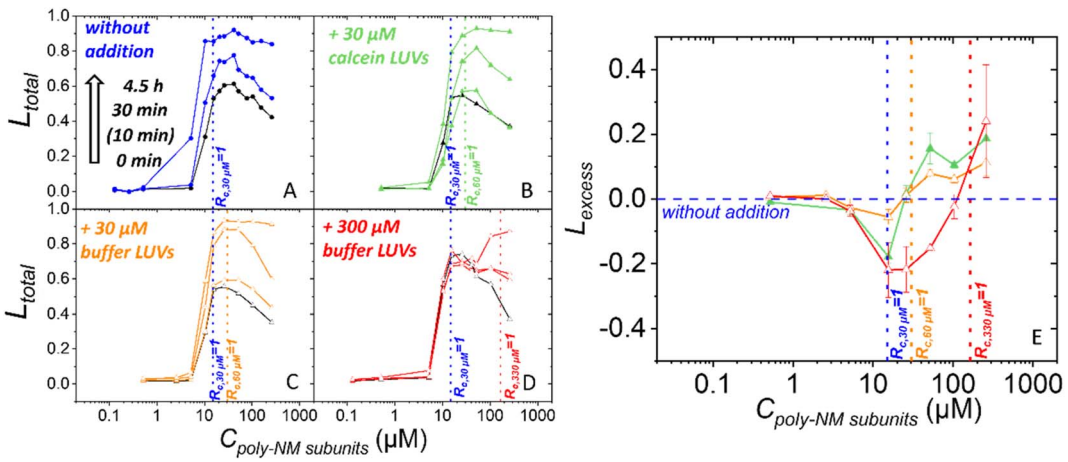

Fig. 6 (A)–(D) Leakage efficiency induced by poly-NM without and with addition of vesicles to preincubated polymer-vesicle samples. (A) Standard L_{total} of 30 μM POPE/POPG (1 : 1) LUVs without additional LUVs (blue). (B) Leakage with addition of 30 μM calcein-filled LUVs (green). (C) Leakage with addition of 30 μM buffer-filled LUVs (orange). (D) Leakage with addition of 300 μM buffer-filled LUVs (red). Various incubation times are indicated relative to the time of addition. Black data represent the leakage just before the addition of LUVs. (E) Summary of excess leakage (L_{excess}) (normalized to the original leakage without additional vesicles) 30 min after the addition of buffer-filled (orange and red) or calcein-filled (green) vesicles to POPE/POPG vesicles preincubated with poly-NM for 30 min. Lines are guides to the eye and the vertical dotted lines represent the theoretical charge saturation ratio ($R_c = 1$) of different lipid concentrations. Errors bars in (E) reflect standard deviation of 3 experiments. Leakage data in (A) is taken from ref. Shi *et al.* 2021 with permission from the PCCP Owner Societies. (All vesicles POPG/POPE 1 : 1, 25 mM MOPS; 130 mM NaCl; pH 7.0; 25 °C).

Concentration-dependent sequence of apparent aggregation and full leaky fusion. When increasing concentrations of poly-NM are incubated with PE/PG vesicles, there is a noteworthy sequence of apparent vesicle aggregation, leakage, and fusion. Fig. S12† displays an overview of the effects of poly-NM on PE/PG vesicles in the various experiments. Because poly-NM lacks hydrophobic molecular surface, poly-NM probably binds to PE/PG vesicles by electrostatic interactions mediated by the charged aminomethyl groups, involving mainly the charged lipid head groups and less the hydrophobic core of the membrane. Also in other contexts, charge-mediated fusion is observed.[44] Furthermore, we confirmed no interaction (*i.e.* no leakage/lipid mixing/content mixing) of poly-NM with zwitterionic palmitoyl-oleoyl-glycero-phosphocholine (POPC) LUVs (Fig. S11†).

The observable effects of poly-NM on negatively charged PE/PG vesicles start at 0.5 μM. Up to $R_c = 1$, there is apparent aggregation including lipid mixing (I). Just below and close to $R_c = 1$, poly-NM induces both full fusion and leakage in PE/PG vesicles (II). With further increasing poly-NM concentrations, leakage remains constant which results in a plateau (III). Let us discuss these concentration ranges in more detail.

(I) Apparent aggregation involving lipid mixing/fusion intermediates. The activity of the polycation below $R_c = 1$ is probably governed by increasing electrostatic binding and increasing neutralization of the vesicle surface charges leads to colloidal instability and apparent aggregation (Fig. 2 and 5). We observed no indications of full fusion, *i.e.*, neither content mixing nor leakage that would explain why content mixing was not detected (Fig. 4). Therefore, the lipid mixing in this concentration range is attributed to apparent aggregation, even though lipid mixing is not expected with peripheral vesicle contacts.[35] In this case, total lipid mixing can be detected if the adjacent membranes form non-bilayer defects that might resemble fusion intermediates, such as tethers, stalks, or hemifusion diaphragms.[45,46] Alternatively, the exchange of lipids between adjacent membranes through the solution might be facilitated.

In other words, what is observed at poly-NM concentrations below $R_c = 1$ might be regarded as the first steps of fusion: overcoming the electrostatic vesicle–vesicle repulsion and dehydration of the lipid head groups.

(II) Full fusion and leakage. In the absence of leakage, the positive polymer charges completely neutralise the negative charges on the outside of vesicles at a concentration of approximately 7.5 μM. That is, half the concentration of $R_c = 1$ referring to all charged lipids in the outer and (still inaccessible) inner leaflets of the vesicles. At this polycation concentration, there is a relatively sharp onset and steep increase of leakage activity, lipid mixing reaches its theoretical maximum, and maximal content mixing is detected (Fig. 4). Both, leakage and full fusion have occurred.

The local concentration of still entrapped calcein (fluorescence lifetime of entrapped dye) indicates an all-or-none mechanism at short incubation times (Shi *et al.* 2021, Fig. S4B†). That is, some vesicles leak entirely while others retain all their content. Together with the observation of content mixing, the all-or-none leakage indicates that at least some of the fusion events have occurred in a tight fashion. Several theoretical studies suggest that leakage is facilitated in a stalk close to the fusion site, *i.e.*, leakage and fusion are mechanistically coupled, but spatially slightly separate processes so that maybe only one of the fusing vesicles becomes leaky just before full fusion completes.[47–49] This might explain our observation of some leakage upon fusion and limited content mixing. Even after careful corrections (see methods and Fig. S8†), there is a possibility of massive turbidity affecting the content-mixing results at $R_c = 1$ differently from conditions with an excess of polycation above $R_c = 1$.

Assuming the conservation of membrane area, many 100 nm LUVs (many more than 10) must have fused to reach the large vesicle size observed in cryo-TEM. Therefore, the volume of the vesicle lumen must have replenished to yield spherical vesicles (Fig. 2 and S1†), probably by buffer flowing in during the leakage events. Leakage thus might be further favored by multiple fusion events or the multiple fusion events might be possible only because of leakage. There is a possibility that the large membrane structures have formed by connection of several smaller, previously solubilized membrane patches, but this would not explain content mixing.

(III) Above $R_c = 1$, no increased leakage and fusion activity with concentration, but over time. With an excess of positively charged poly-NM, above $R_c = 1$, both leakage and lipid mixing reach a plateau, where an increase in poly-NM concentration does not increase activity. This behavior is likely caused by the predominant electrostatic binding of poly-NM that only increases until the excess of negative charges on vesicles are saturated.

According to our kinetic experiments and as proposed before,[8] both processes, leakage and fusion occur on the timescale of approximately 10 min (Fig. S4, S6 and S7†). However, the leakage plateau rises over time[28] (Fig. S4†), indicating the re-occurrence of leakage events.[50] As proposed before[28] and discussed below on the basis of the behavior of L_{excess}, we think that there is a dynamic binding equilibrium allowing poly-NM to redistribute and apparently induce more leakage over time. Judged by slight increases in lipid mixing, too (Fig. S6†), the fusion process might continue. Continuing fusion of filled and equilibrated vesicles or if vesicles become larger when replenishing their internal volume after fusion might also account for the gradual increase in fluorescence lifetime of entrapped calcein (apparent gradual dilution of entrapped calcein) for longer incubation times (Fig. S4B†).[28]

The apparent loss of content mixing signal above $R_c = 1$ is a logical consequence of the pronounced leakage activity of poly-NM, as both ANTS and DPX might become too diluted to cause a signal change.

This sequence of events points to a correlation of full fusion and leakage, but is no proof. We further investigated leakage behavior while either preventing bilayer–bilayer contacts by incorporating PEG-lipids or by increasing the likeliness of bilayer–bilayer contacts at increased vesicle concentrations.

Steric shielding with PEG-lipids corroborates a role of bilayer–bilayer contacts in leakage. 4 mol% PEG-lipids suffice to completely impede apparent vesicle aggregation, lipid and

content mixing, and vesicle leakage (Fig. 2, 4 and 5). Thus, fusion seems correlated to leakage induced by poly-NM. Notably, both the fast leakage, but also the apparent long-term increase in leakage are eliminated (Fig. S4†). There seems to be no additional fusion-independent slow leakage mechanism.

While it is relatively easy to envision that aggregation and fusion are inhibited by sterical shielding, it is more difficult to explain the pronounced effect of PEG-lipids on leakage. We excluded several possibilities: the slight changes in binding of poly-NM to PEG-vesicles compared to PEG-free vesicles can be explained by access to the inner layer lipids and should not account for a complete loss of leakage activity (Fig. 3). Theoretically, PEG-chains might somehow interfere with the formation of a transmembrane pore. Still, we consider leaky fusion as the most probable leakage mechanism and tested specifically for that by increasing the vesicle concentration during leakage experiments.

Leakage increases with the likeliness of bilayer–bilayer contacts. The addition of further vesicles to a sample preincubated with polymers answers two questions: first, do the polymers redistribute also over the then newly added vesicles, or are they sequestered by the preincubated vesicles? Second, do increased bilayer–bilayer contacts (by increasing the vesicle number) increase leakage, which would further corroborate leaky fusion?

When increasing the lipid concentration, *i.e.,* the probability of bilayer–bilayer contacts, we need to keep in mind that the lipid/polymer ratio and charge ratio will change as well. Assuming that the polymer is redistributed after addition of vesicles, the bound polymer might not suffice for neutralization and induction of leaky fusion (Fig. S12†). Indeed, for all addition experiments, we found less leakage than expected ($L_{excess} < 0$) in the range between the $R_{c,30\ \mu M} = 1$ in the preincubated samples and the new $R_{c,60\ \mu M \text{ or } 330\ \mu M} = 1$ for the increased lipid concentration (Fig. 6). In conclusion, there is a dynamic binding equilibrium of polymers.

Regarding the leakage mechanism, leaky fusion should increase with the number of vesicles per volume at or above $R_c = 1$. Indeed, additional leakage is induced as expected starting at $R_{c,60\ \mu M} = 1$ or $R_{c,330\ \mu M} = 1$, respectively (Fig. 6). Also, particle sizes become huge and variable at this condition (Fig. S10†). What is more, both, before and after vesicle addition, leakage and excess leakage occur with a similar time course expected for fusion to occur.[12] This indicates that the leakage mechanism does not change with vesicle addition and is in line with the hypothesized leaky fusion as leakage mechanism before addition and also after addition of vesicles.

Relevance for other antimicrobials and membrane-active compounds. Let us first compare poly-NM and the structurally related, more hydrophobic MM:CO, a highly active, but unselective polycation.[22,27,28] Strikingly, there are strong similarities in the leakage behavior induced by poly-NM and MM:CO that turned out to be caused by totally different processes. For example, both, poly-NM and MM:CO induce relatively fast leakage at the same polycation concentration in POPE/POPG vesicles. Both polymers also cause apparent vesicle aggregation and fusion. To our surprise, the stronger fusogen MM:CO causes leakage first by asymmetric packing stress[22] and not by leaky fusion like poly-NM. Similarly, peptides synthetically evolved for triggered release are fusogenic, but induce leakage independent of fusion.[51]

For cell-penetrating, arginine-rich peptides interacting with phosphatidylocholine/PE/bis(monoacylglycerol)phosphate or more complex lipids mixtures, not only fusion and leakage, but also concomitant inhibition or increase of fusion and leakage, *i.e.*, leaky fusion were observed.[12,13] A mixture of magainin 2 and PGLa induces morphological membrane changes resembling fusion that might explain their leakage activity.[52] Also, several other synthetic mimics of antimicrobial peptides predominantly containing positively charged subunits and little hydrophobic molecular surface induce leakage behavior that would be in line with leaky fusions, in particular a plateau in leakage: diamine SMAMP with TOCL/POPE vesicles,[53] poly-NM or poly-MM with YPLE vesicles.[27] More information about possible fusion activity is still missing for these polycations that predominantly bind to negatively charged vesicles by electrostatic interactions. The examples also suggest that the plateau-leakage behavior and potentially leaky fusion is not a property of PE/PG 1 : 1 mixtures. Most examples contain a lipid preferring negative spontaneous curvature (POPE, cardiolipin, or BMP).

There are more reported indications of turbidity/fusion/aggregation activity induced by antimicrobial peptides or polymers[7,9,54,55] and many more where increased particle sizes were not explicitly tested for. It might be helpful to check for leaky fusion also in these cases.

Conclusion

For the antimicrobial polycation poly-NM acting on negatively charged POPE/POPG model vesicles, we established leaky vesicle fusion as the most likely mechanism of membrane permeabilization. Having in mind that the activity of polycations on oppositely charged vesicles relies on unspecific physical–chemical effects, our findings are probably of more general relevance, especially for less hydrophobic polycations and lipids preferring negative spontaneous curvature.

Let us consider two types of implications: first, vesicle aggregation and fusion might cause experimental problems and might remain unnoticed and leaky fusion is difficult to prove and to distinguish from other leakage mechanisms. Second, the role of these types of membrane perturbations (*e.g.* leaky fusion) for the understanding and judgment of antimicrobial activity needs to be refined.

Experimental implications of leaky fusion

We demonstrated here, that when increased particle sizes are suspected, identification of the process can determine whether aggregation or fusion are indeed just side-effects or do play a more significant role.

Interestingly, as in the present case, increases in particle size can have different causes. Besides vesicle aggregation with only

peripheral membrane contacts, there is apparent aggregation involving lipid exchange, thus potentially resembling fusion-intermediates. Furthermore, there is full vesicle fusion and leaky fusion.

As we have demonstrated in the current and a previous paper on a related polymer MM:CO,[22] clearly disentangling leakage and fusion can be difficult. If concomitant membrane leakage occurs, the combination of the lipid mixing and content mixing assays might not suffice to unambiguously identify apparent aggregation, and full fusion.[37] Complementary tests (*e.g.* addition of PEG-lipids/more vesicles) and methods (*e.g.* microscopy) may help. It is helpful to keep in mind the different conditions of each experiment. Most importantly, the absolute lipid concentration influences polymer or peptide partitioning to lipid membranes.[56–58]

Unfortunately, the increase in particle size by aggregation or fusion also causes turbidity/sedimentation and changes in light scattering, which requires meticulous corrections and careful data interpretation to avoid artefacts in experimental outcomes.

Relevance of leaky fusion in antimicrobial treatment, biology, and therapeutic applications

All these corrections and controls in model studies are unfavourable. Even worse, as in the case of poly-NM, membrane permeabilization in model vesicles might be solely caused by leaky fusion. In microbes, direct membrane–membrane contacts and, in turn, membrane fusion between cells are prevented by the outer cell wall components. Therefore, leaky fusion as mechanism of permeabilization is not directly relevant to antibacterial activity.

However, leaky fusion and induced fusion might still be relevant in an indirect way or contribute to a multi-hit strategy.[59,60] For example, even early fusion intermediates involve a propensity for non-bilayer structures or local curvature which probably disturbs membrane function or the function of membrane proteins.[14] Additionally, (pathogenic) fungi contain intracellular membrane compartments whose aggregation and fusion properties might be changed by polycations. This might explain the high activity of poly-NM for fungi such as *C. albicans* or *C. neoformans* (<10 μM) compared to bacteria (in the range of 10–100 μM) or compared to the more hydrophobic MM:CO polycation.[29]

Excluding leaky fusion is crucial for a meaningful comparison of model studies aiming at the mechanism of action to microbiological activity or for screening compounds designed to induce membrane permeabilization.

Also in other contexts, comprehensively understanding membrane permeabilization, membrane aggregation, fusion intermediates, full fusion, and leaky fusion is advantageous. For instance, fusion is important in cell entry of enveloped viruses or other pathogens, vesicle trafficking, the synaptic process, fertilization, drug delivery by liposomes, *etc.*

A good understanding and fine-tuning regarding the onset and interplay of leakage and fusion holds the potential to improve membrane-active antimicrobials and membrane-active compounds for therapy.

Author contributions

SS performed experiments. HF and MH prepared the leakage protocol. SS and MH conceived experiments, performed data analysis and wrote the manuscript.

Conflicts of interest

There are no conflicts to declare.

Acknowledgements

We gratefully acknowledge the lab of Runhui Liu (East China University of Science and Technology, Shanghai, China) for kindly providing poly-NM. At Freiburg University, we thank Mrs Sabine Barnert for cryo-TEM experiments and Anja Markl for help with the lipid mixing and content mixing assay. We acknowledge access to instrumentation and input to the leakage protocol by the Heerklotz lab. Main funding was contributed by the German Research Foundation (DFG 415894560) to MH and SS.

References

1 D. Volodkin, V. Ball, P. Schaaf, J.-C. Voegel and H. Mohwald, Complexation of phosphocholine liposomes with polylysine. Stabilization by surface coverage versus aggregation, *Biochim. Biophys. Acta*, 2007, **1768**, 280–290.
2 T. M. Domingues, B. Mattei, J. Seelig, K. R. Perez, A. Miranda and K. A. Riske, Interaction of the Antimicrobial Peptide Gomesin with Model Membranes: A Calorimetric Study, *Langmuir*, 2013, **29**, 8609–8618.
3 Y. G. Smirnova, H. J. Risselada and M. Müller, Thermodynamically reversible paths of the first fusion intermediate reveal an important role for membrane anchors of fusion proteins, *Proc. Natl. Acad. Sci. U. S. A.*, 2019, **116**, 2571–2576.
4 A. N. D. Stefanovic, M. M. A. E. Claessens, C. Blum and V. Subramaniam, Alpha-Synuclein Amyloid Oligomers Act as Multivalent Nanoparticles to Cause Hemifusion in Negatively Charged Vesicles, *Small*, 2015, **11**, 2257–2262.
5 S. Nir, F. Nicol and F. C. Szoka, Surface aggregation and membrane penetration by peptides: relation to pore formation and fusion, *Mol. Membr. Biol.*, 1999, **16**, 95–101.
6 R. A. Parente, S. Nir and F. C. Szoka, pH-dependent fusion of phosphatidylcholine small vesicles. Induction by a synthetic amphipathic peptide, *J. Biol. Chem.*, 1988, **263**, 4724–4730.
7 L. Marx, E. F. Semeraro, J. Mandl, J. Kremser, M. P. Frewein, N. Malanovic, K. Lohner and G. Pabst, Bridging the Antimicrobial Activity of Two Lactoferricin Derivatives in E. coli and Lipid-Only Membranes, *Front. Med. Technol.*, 2021, **3**, 625975.
8 W. C. Wimley and K. Hristova, The Mechanism of Membrane Permeabilization by Peptides: Still an Enigma, *Aust. J. Chem.*, 2019, **73**, 96–103.
9 G. D. Eytan, R. Broza and Y. Shalitin, Gramicidin S and dodecylamine induce leakage and fusion of membranes at

micromolar concentrations, *Biochim. Biophys. Acta*, 1988, **937**, 387–397.
10 G. Fujii, M. E. Selsted and D. Eisenberg, Defensins promote fusion and lysis of negatively charged membranes, *Protein Sci.*, 1993, **2**, 1301–1312.
11 X. Xia, F. Zhang, P.-C. Shaw and S.-F. Sui, Trichosanthin induces leakage and membrane fusion of liposome, *IUBMB Life*, 2003, **55**, 681–687.
12 S.-T. Yang, E. Zaitseva, L. V. Chernomordik and K. Melikov, Cell-penetrating peptide induces leaky fusion of liposomes containing late endosome-specific anionic lipid, *Biophys. J.*, 2010, **99**, 2525–2533.
13 D. J. Brock, H. Kondow-McConaghy, J. Allen, Z. Brkljača, L. Kustigian, M. Jiang, J. Zhang, H. Rye, M. Vazdar and J.-P. Pellois, Mechanism of Cell Penetration by Permeabilization of Late Endosomes: Interplay between a Multivalent TAT Peptide and Bis(monoacylglycero) phosphate, *Cell Chem. Biol.*, 2020, **27**, 1296–1307.
14 K. Scheinpflug, M. Wenzel, O. Krylova, J. E. Bandow, M. Dathe and H. Strahl, Antimicrobial peptide cWFW kills by combining lipid phase separation with autolysis, *Sci. Rep.*, 2017, **7**, 44332.
15 R. M. Epand and R. F. Epand, Lipid domains in bacterial membranes and the action of antimicrobial agents, *Biochim. Biophys. Acta*, 2009, **1788**, 289–294.
16 S. Finger, A. Kerth, M. Dathe and A. Blume, The efficacy of trivalent cyclic hexapeptides to induce lipid clustering in PG/PE membranes correlates with their antimicrobial activity, *Biochim. Biophys. Acta*, 2015, **1848**, 2998–3006.
17 S. Guha, J. Ghimire, E. Wu and W. C. Wimley, Mechanistic Landscape of Membrane-Permeabilizing Peptides, *Chem. Rev.*, 2019, **119**, 6040–6085.
18 A. S. Ladokhin, W. C. Wimley and S. H. White, Leakage of membrane vesicle contents: determination of mechanism using fluorescence requenching, *Biophys. J.*, 1995, **69**, 1964–1971.
19 H. Patel, C. Tscheka and H. Heerklotz, Characterizing vesicle leakage by fluorescence lifetime measurements, *Soft Matter*, 2009, **5**, 2849.
20 A. Witkowska, L. P. Heinz, H. Grubmüller and R. Jahn, Tight docking of membranes before fusion represents a metastable state with unique properties, *Nat. Commun.*, 2021, **12**, 3606.
21 S. L. Leikin, M. M. Kozlov, L. V. Chernomordik, V. S. Markin and Y. A. Chizmadzhev, Membrane fusion: overcoming of the hydration barrier and local restructuring, *J. Theor. Biol.*, 1987, **129**, 411–425.
22 S. Shi, A. M. Markl, Z. Lu, R. Liu and M. Hoernke, Interplay of Fusion, Leakage, and Electrostatic Lipid Clustering: Membrane Perturbations by a Hydrophobic Antimicrobial Polycation, *Langmuir*, 2022, **38**, 2379–2391.
23 H. Heerklotz, Membrane Stress and Permeabilization Induced by Asymmetric Incorporation of Compounds, *Biophys. J.*, 2001, **81**, 184–195.
24 S. Esteban-Martín, H. J. Risselada, J. Salgado and S. J. Marrink, Stability of Asymmetric Lipid Bilayers Assessed by Molecular Dynamics Simulations, *J. Am. Chem. Soc.*, 2009, **131**, 15194–15202.
25 H. Takahashi, G. A. Caputo, S. Vemparala and K. Kuroda, Synthetic Random Copolymers as a Molecular Platform to Mimic Host-Defense Antimicrobial Peptides, *Bioconjugate Chem.*, 2017, **28**, 1340–1350.
26 C. Ergene, K. Yasuhara and E. F. Palermo, Biomimetic antimicrobial polymers: recent advances in molecular design, *Polym. Chem.*, 2018, **9**, 2407–2427.
27 S. G. Hovakeemian, R. Liu, S. H. Gellman and H. Heerklotz, Correlating antimicrobial activity and model membrane leakage induced by nylon-3 polymers and detergents, *Soft Matter*, 2015, **11**, 6840–6851.
28 S. Shi, N. Quarta, H. Zhang, Z. Lu, M. Hof, R. Šachl, R. Liu and M. Hoernke, Hidden complexity in membrane permeabilization behavior of antimicrobial polycations, *Phys. Chem. Chem. Phys.*, 2021, **23**, 1475–1488.
29 R. Liu, X. Chen, S. P. Falk, B. P. Mowery, A. J. Karlsson, B. Weisblum, S. P. Palecek, K. S. Masters and S. H. Gellman, Structure-activity relationships among antifungal nylon-3 polymers: identification of materials active against drug-resistant strains of Candida albicans, *J. Am. Chem. Soc.*, 2014, **136**, 4333–4342.
30 R. Liu, X. Chen, Z. Hayouka, S. Chakraborty, S. P. Falk, B. Weisblum, K. S. Masters and S. H. Gellman, Nylon-3 polymers with selective antifungal activity, *J. Am. Chem. Soc.*, 2013, **135**, 5270–5273.
31 G. R. Bartlett, Phosphorus Assay in Column Chromatography, *J. Biol. Chem.*, 1959, **234**, 466–468.
32 S. Keller, C. Vargas, H. Zhao, G. Piszczek, C. A. Brautigam and P. Schuck, High-precision isothermal titration calorimetry with automated peak-shape analysis, *Anal. Chem.*, 2012, **84**, 5066–5073.
33 T. H. Scheuermann and C. A. Brautigam, High-precision, automated integration of multiple isothermal titration calorimetric thermograms: new features of NITPIC, *Methods*, 2015, **76**, 87–98.
34 D. K. Struck, D. Hoekstra and R. E. Pagano, Use of resonance energy transfer to monitor membrane fusion, *Biochemistry*, 1981, **20**, 4093–4099.
35 N. Düzgüneş, T. M. Allen, J. Fedor and D. Papahadjopoulos, Lipid mixing during membrane aggregation and fusion: why fusion assays disagree, *Biochemistry*, 1987, **26**, 8435–8442.
36 H. Ellens, J. Bentz and F. C. Szoka, H^+- and Ca^{2+}-induced fusion and destabilization of liposomes, *Biochemistry*, 1985, **24**, 3099–3106.
37 A. V. Villar, A. Alonso and F. M. Goñi, Leaky vesicle fusion induced by phosphatidylinositol-specific phospholipase C: observation of mixing of vesicular inner monolayers, *Biochemistry*, 2000, **39**, 14012–14018.
38 J. E. Cummings and T. K. Vanderlick, Aggregation and hemi-fusion of anionic vesicles induced by the antimicrobial peptide cryptdin-4, *Biochim. Biophys. Acta*, 2007, **1768**, 1796–1804.
39 J. W. Holland, C. Hui, P. R. Cullis and T. D. Madden, Poly(ethylene glycol)–Lipid Conjugates Regulate the Calcium-Induced Fusion of Liposomes Composed of

Phosphatidylethanolamine and Phosphatidylserine, *Biochemistry*, 1996, **35**, 2618–2624.
40 A. K. Kenworthy, K. Hristova, D. Needham and T. J. McIntosh, Range and magnitude of the steric pressure between bilayers containing phospholipids with covalently attached poly(ethylene glycol), *Biophys. J.*, 1995, **68**, 1921–1936.
41 S. W. Hui, T. L. Kuhl, Y. Q. Guo and J. Israelachvili, Use of poly(ethylene glycol) to control cell aggregation and fusion, *Colloids Surf., B*, 1999, **14**, 213–222.
42 P. G. de Gennes, Polymers at an interface; a simplified view, *Adv. Colloid Interface Sci.*, 1987, **27**, 189–209.
43 S. Rex, J. Bian, J. R. Silvius and M. Lafleur, The presence of PEG-lipids in liposomes does not reduce melittin binding but decreases melittin-induced leakage, *Biochim. Biophys. Acta*, 2002, **1558**, 211–221.
44 R. B. Lira, T. Robinson, R. Dimova and K. A. Riske, Highly Efficient Protein-free Membrane Fusion: A Giant Vesicle Study, *Biophys. J.*, 2019, **116**, 79–91.
45 G. B. Melikyan, Driving a wedge between viral lipids blocks infection, *Proc. Natl. Acad. Sci. U. S. A.*, 2010, **107**, 17069–17070.
46 S. Mondal Roy and M. Sarkar, Membrane fusion induced by small molecules and ions, *J. Lipids*, 2011, **2011**, 528784.
47 B. Bu, M. Crowe, J. Diao, B. Ji and D. Li, Cholesterol suppresses membrane leakage by decreasing water penetrability, *Soft Matter*, 2018, **14**, 5277–5282.
48 H. J. Risselada, G. Bubnis and H. Grubmüller, Expansion of the fusion stalk and its implication for biological membrane fusion, *Proc. Natl. Acad. Sci. U. S. A.*, 2014, **111**, 11043–11048.
49 K. Katsov, M. Müller and M. Schick, Field theoretic study of bilayer membrane fusion: II. Mechanism of a stalk-hole complex, *Biophys. J.*, 2006, **90**, 915–926.
50 C. Mazzuca, B. Orioni, M. Coletta, F. Formaggio, C. Toniolo, G. Maulucci, M. de Spirito, B. Pispisa, M. Venanzi and L. Stella, Fluctuations and the rate-limiting step of peptide-induced membrane leakage, *Biophys. J.*, 2010, **99**, 1791–1800.
51 L. Sun, K. Hristova and W. C. Wimley, Membrane-selective nanoscale pores in liposomes by a synthetically evolved peptide: implications for triggered release, *Nanoscale*, 2021, **13**, 12185–12197.
52 I. Kabelka, M. Pachler, S. Prévost, I. Letofsky-Papst, K. Lohner, G. Pabst and R. Vácha, Magainin 2 and PGLa in Bacterial Membrane Mimics II: Membrane Fusion and Sponge Phase Formation, *Biophys. J.*, 2020, **118**, 612–623.
53 A. Stulz, A. Vogt, J. S. Saar, L. Akil, K. Lienkamp and M. Hoernke, Quantified Membrane Permeabilization Indicates the Lipid Selectivity of Membrane-Active Antimicrobials, *Langmuir*, 2019, **35**, 16366–16376.
54 M. Makowski, M. R. Felício, I. C. M. Fensterseifer, O. L. Franco, N. C. Santos and S. Gonçalves, EcDBS1R4, an Antimicrobial Peptide Effective against Escherichia coli with In Vitro Fusogenic Ability, *Int. J. Mol. Sci.*, 2020, **21**, 9104.
55 S. L. Hanna, J. L. Huang, A. J. Swinton, G. A. Caputo and T. D. Vaden, Synergistic effects of polymyxin and ionic liquids on lipid vesicle membrane stability and aggregation, *Biophys. Chem.*, 2017, **227**, 1–7.
56 H. Heerklotz and S. Keller, How membrane partitioning modulates receptor activation: parallel versus serial effects of hydrophobic ligands, *Biophys. J.*, 2013, **105**, 2607–2610.
57 D. Roversi, V. Luca, S. Aureli, Y. Park, M. L. Mangoni and L. Stella, How many antimicrobial peptide molecules kill a bacterium? The case of PMAP-23, *ACS Chem. Biol.*, 2014, **9**, 2003–2007.
58 F. Savini, V. Luca, A. Bocedi, R. Massoud, Y. Park, M. L. Mangoni and L. Stella, Cell-Density Dependence of Host-Defense Peptide Activity and Selectivity in the Presence of Host Cells, *ACS Chem. Biol.*, 2017, **12**, 52–56.
59 Y. Shai, Mode of action of membrane active antimicrobial peptides, *Biopolymers*, 2002, **66**, 236–248.
60 R. E. Hancock and G. Diamond, The role of cationic antimicrobial peptides in innate host defences, *Trends Microbiol.*, 2000, **8**, 402–410.